Lysosomal integral membrane protein 2 is a novel component of the cardiac intercalated disc and vital for load-induced cardiac myocyte hypertrophy

Blanche Schroen,[1] Joost J. Leenders,[1] Arie van Erk,[1] Anne T. Bertrand,[3] Mirjam van Loon,[1] Rick E. van Leeuwen,[1] Nard Kubben,[1] Rudy F. Duisters,[1] Mark W. Schellings,[1] Ben J. Janssen,[2] Jacques J. Debets,[2] Michael Schwake,[4] Morten A. Høydal,[5] Stephane Heymans,[1] Paul Saftig,[4] and Yigal M. Pinto[1]

[1]Department of Experimental and Molecular Cardiology and [2]Department of Pharmacology/CARIM, University of Maastricht, 6202 AZ Maastricht, Netherlands
[3]Hubrecht Laboratory and Interuniversity Cardiology Institute Netherlands, Royal Netherlands Academy of Arts and Sciences, 3584 CT Utrecht, Netherlands
[4]Biochemisches Institut, Universität Kiel, 24098 Kiel, Germany
[5]Department of Circulation and Medical Imaging, Norwegian University of Science and Technology, NO-7491 Trondheim, Norway

The intercalated disc (ID) of cardiac myocytes is emerging as a crucial structure in the heart. Loss of ID proteins like N-cadherin causes lethal cardiac abnormalities, and mutations in ID proteins cause human cardiomyopathy. A comprehensive screen for novel mechanisms in failing hearts demonstrated that expression of the lysosomal integral membrane protein 2 (LIMP-2) is increased in cardiac hypertrophy and heart failure in both rat and human myocardium. Complete loss of LIMP-2 in genetically engineered mice did not affect cardiac development; however, these LIMP-2 null mice failed to mount a hypertrophic response to increased blood pressure but developed cardiomyopathy. Disturbed cadherin localization in these hearts suggested that LIMP-2 has important functions outside lysosomes. Indeed, we also find LIMP-2 in the ID, where it associates with cadherin. RNAi-mediated knockdown of LIMP-2 decreases the binding of phosphorylated β-catenin to cadherin, whereas overexpression of LIMP-2 has the opposite effect.

Collectively, our data show that LIMP-2 is crucial to mount the adaptive hypertrophic response to cardiac loading. We demonstrate a novel role for LIMP-2 as an important mediator of the ID.

CORRESPONDENCE
Yigal M. Pinto:
Y.Pinto@cardio.azm.nl

Abbreviations used: ANF, atrial natriuretic factor; Ang, angiotensin; aska, α-skeletal actin; BNP, brain natriuretic peptide; HF, heart failure; ID, intercalated disc; IP, immunoprecipitation; LIMP-2, lysosomal integral membrane protein 2; LV, left ventricle; RCM, rat ventricular cardiac myocyte; shLIMP-2, short-hairpin RNA against LIMP-2; shRNA, short-hairpin RNA; TSP, thrombospondin.

Chronic cardiac loading as occurs during long-standing hypertension induces cardiac hypertrophy, which often progresses to left ventricle (LV) dysfunction and overt heart failure (HF). The molecular changes that precede and herald this transition from hypertrophy toward HF are incompletely understood (1).

The intercalated disc (ID) of cardiac myocytes has emerged as a crucial structure in the heart. The cardiac ID consists of three major structures: gap junctions, adherens junctions, and desmosomes. In dilated cardiomyopathy, the number of gap junctions is decreased while the adherens junctions increase, leading to reduced cardiac communication and increased stiffness (2). An important role for ID structure is further demonstrated by the fact that complete loss of ID proteins like N-cadherin, plakoglobin, and β-catenin (3–6) is lethal. Moreover, mutations in ID proteins like desmoplakin, desmoglobin, plakoglobin, and plakophilin-2 (7–9) cause human cardiomyopathies. However, factors that more subtly modulate the ID have not yet been described.

We have previously reported on the unique propensity of the homozygous hypertensive transgenic rat TGR(mRen-2) 27 (Ren-2). A proportion of these rats rapidly progresses toward HF,

The online version of this article contains supplemental material. Supplemental material can be found at: http://doi.org/10.1084/jem.20070145

whereas the other rats remain compensated for a prolonged time (10). Obtaining minute LV biopsies in these Ren-2 rats in an early stage of compensated LV hypertrophy allowed us to identify molecular changes that precede the transition toward HF, such as increased expression of thrombospondin (TSP)2 and galectin-3 (10, 11). We recently were able to use these minute LV biopsies to reliably obtain comprehensive gene expression profiles from the LV. We showed that linear amplification allowed us to retain a highly representative gene expression profile comparable to that obtained from a whole heart homogenate (12). Therefore, obtaining Ren-2 rat LV biopsies now allowed us to search in a more comprehensive manner for novel molecular mechanisms that precede the transition toward HF. We compared gene expression profiles obtained from hypertrophic hearts that either progressed to HF or remained compensated. Among the 143 genes that were differentially regulated in failure-prone hypertrophied hearts, lysosomal integral membrane protein 2 (LIMP-2) was up-regulated in failure-prone hearts. LIMP-2 was up-regulated quickly in the heart upon pressure loading. LIMP-2 KO mice lacked a normal hypertrophic response to pressure loading with angiotensin (Ang)II, but quickly developed dilated cardiomyopathy accompanied by a disturbed structure of the ID. In human hearts as well as in cardiac myocytes in vitro, LIMP-2 was found to interact with N-cadherin at the site of the ID. We propose that LIMP-2 is a novel regulator of the cardiac ID, and that it is crucial in the development of adaptive cardiac hypertrophy possibly through its effects on the binding of the two ID members β-catenin and N-cadherin.

RESULTS

Gene expression profile of failure-prone LV hypertrophy

We obtained cardiac biopsies in 10 homozygous Ren-2 rats at a stage of compensated LV hypertrophy at 10 wk of age. Four rats rapidly progressed toward HF within 5 wk after the biopsy was taken, whereas the remaining six rats remained compensated for 11 wk after biopsy (Fig. 1 A). After linear T7-based amplification and subsequent Affymetrix RAE230 2.0 gene expression analysis of these biopsies (GEO accession number GSE4286), we identified 181 differentially expressed genes that were up- or down-regulated exclusively in the hypertrophied hearts that progressed toward HF (Table S1, available at http://www.jem.org/cgi/content/full/jem.20070145/DC1). LIMP-2, a lysosomal membrane protein, was one of the up-regulated mRNAs in HF-prone rats (Fig. 1 B) and is of particular interest given its ability to interact with TSP1 (13) and TSP2 (not depicted), the latter of which we have shown to be crucial in the transition from hypertrophy toward HF (10). Fig. 1 C shows that LIMP-2 protein also has a role in end-stage HF in Ren-2 rats.

AngII induces dilated cardiomyopathy in LIMP-2 KO mice

Because loss-of-function mutations in lysosomal proteins have been linked to HF (14–16), we further investigated the role of LIMP-2 in a mouse model of AngII-induced hypertension. AngII was given subcutaneously for 2 and 4 wk to

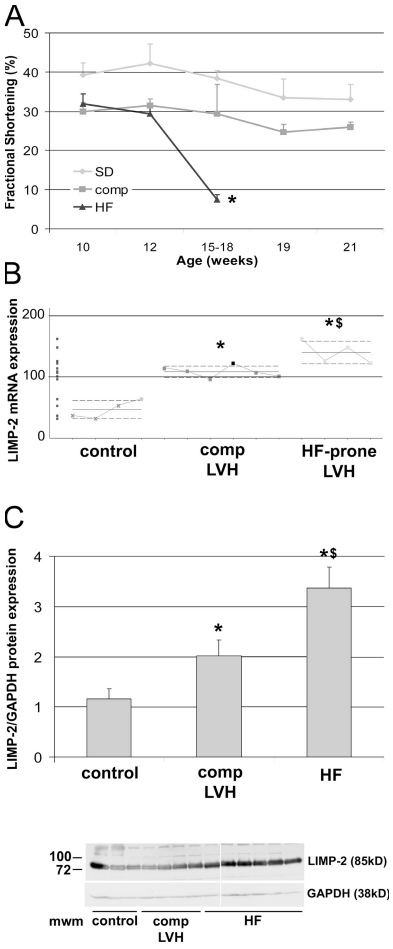

Figure 1. Increased expression of LIMP-2 in Ren-2 rats. An LV biopsy was taken at 10 wk of age, when Ren-2 rats exhibit comparable cardiac hypertrophy (reference 10) and fractional shortening cannot distinguish between rats that will progress to HF or those that will stay compensated (A). Between 15 and 18 wk of age, part of the Ren-2 rats progressed to HF, whereas the remainder stayed compensated until they were killed at 21 wk of age *, $P < 10^{-5}$. In 10-wk-old hypertrophic Ren-2 rats, microarray analysis showed specific overexpression of LIMP-2 mRNA in failure-prone rats (HF-prone LVH; $n = 4$) as compared with the hypertrophied hearts that remained compensated (comp LVH; $n = 6$) and to controls ($n = 4$) (B). LIMP-2 protein was up-regulated in end-stage failing Ren-2 rats (HF; $n = 9$) as compared with compensated Ren-2 rats (comp; $n = 6$) and control rats ($n = 6$) (C). *, $P < 0.05$ versus control; **, $P < 0.01$ versus control; $, $P < 0.05$ versus comp; Mwm, molecular weight marker; au, arbitrary units.

LIMP-2 KO and control mice. AngII treatment resulted in a 29.8 and 30.2% increase in LV mass index in WT mice after 2 and 4 wk, respectively, but the hypertrophic response was virtually absent in the AngII-treated LIMP-2 KO mice (8.7% increase in LV mass index after 2 wk and 13.7% after 4 wk; $P < 0.01$ vs. AngII-treated WT mice; Fig. 2 A and Table S2, which is available at http://www.jem.org/cgi/content/full/jem.20070145/DC1). This was confirmed by measurement of individual cardiac myocyte area after 4 wk of AngII treatment. LV myocyte area was significantly smaller in AngII-treated

KO mice than in AngII-treated WT controls (myocyte area in arbitrary units: 264 ± 42 in AngII-treated KO mice vs. 308 ± 14 in AngII-treated WTs; $P < 0.01$). In addition, although AngII induced comparable increases in perivascular fibrosis in LIMP-2 KO and WT mice (not depicted), 4 wk of AngII treatment induced a massive interstitial fibrotic response in the LVs of LIMP-2 KO mice as opposed to WT control littermates (interstitial fibrosis: 15.0 ± 6.0% in AngII-treated KO mice vs. 3.8 ± 1.7% in AngII-treated controls; $P < 0.05$; Fig. 3). This increased interstitial fibrosis in AngII-treated KO mice did not occur after 2 wk of AngII treatment (interstitial fibrosis: 4.7 ± 1.1% in AngII-treated KO mice vs. 4.8 ± 1.6% in AngII-treated controls; Fig. 3). Immunohistochemical staining for desmin showed altered internal architecture of cardiac myocytes in AngII-treated LIMP-2 null mice (Fig. 4 and Fig. S1).

We ensured that AngII induced a similar blood pressure response in both WT and KO mice (Fig. 2 B). Despite decreased LV hypertrophy, LIMP-2 null mice demonstrated a normal response of the classical markers for hypertrophy brain natriuretic peptide (BNP) and atrial natriuretic factor (ANF; Fig. 2 C), suggesting that the hypertrophic gene expression program was normally initiated upon AngII treatment. In contrast, the structural cellular hypertrophy marker α-skeletal actin (aska) was induced to a significantly lesser extent in AngII-treated LIMP-2 KOs as compared with AngII-treated

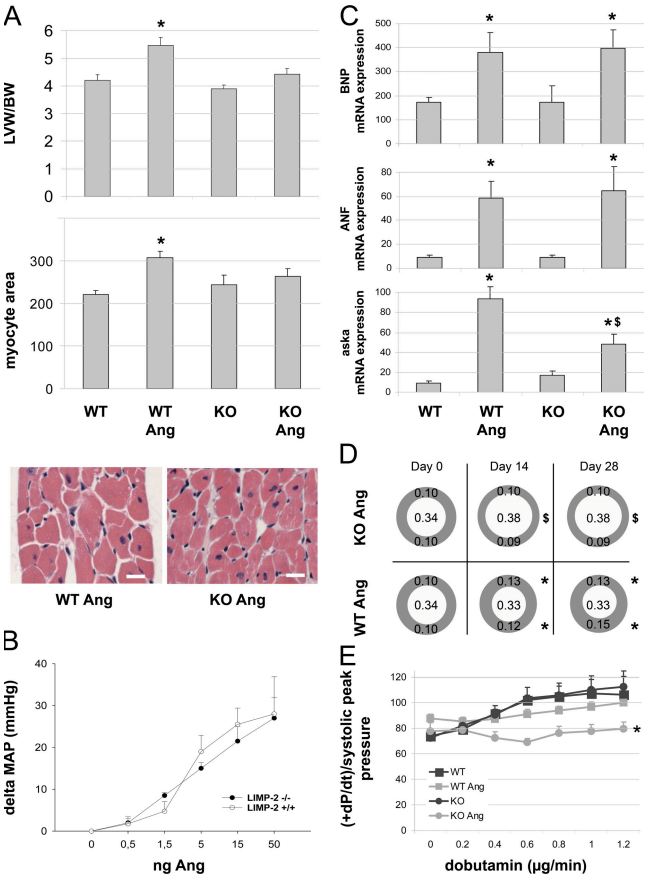

Figure 2. AngII treatment in LIMP-2 KO (KO Ang) mice induces dilated cardiomyopathy. AngII increased LV weight and myocyte area in WT mice ($n = 14$) but not in KO mice ($n = 14$; *, $P < 0.01$ versus WT; $n = 8$) (A). Bars, 50 µm. LIMP-2 KO ($n = 3$) and WT ($n = 4$) mice showed comparable blood pressure responses to AngII (B). BNP, ANF, and aska mRNAs were induced in WT Ang and KO Ang (*, $P < 0.05$ vs. baseline; $n = 4$), but aska to a significantly lesser extend in KO Ang ($, $P < 0.05$ vs. WT Ang) (C). Echocardiography shows hypertrophied LV walls in WT Ang at days 14 and 28, whereas KOs did not show hypertrophy but were dilated (*, $P < 0.005$ vs. baseline and KO Ang; $, $P < 0.005$ vs. baseline and WT Ang; all groups, $n \geq 9$) (D). β-adrenergic response to dobutamin was decreased in KO Ang mice (WT and KO, $n = 4$; WT Ang, $n = 14$; KO Ang, $n = 9$; *, $P < 0.005$) (E). LVW/BW, LV weight corrected for body weight.

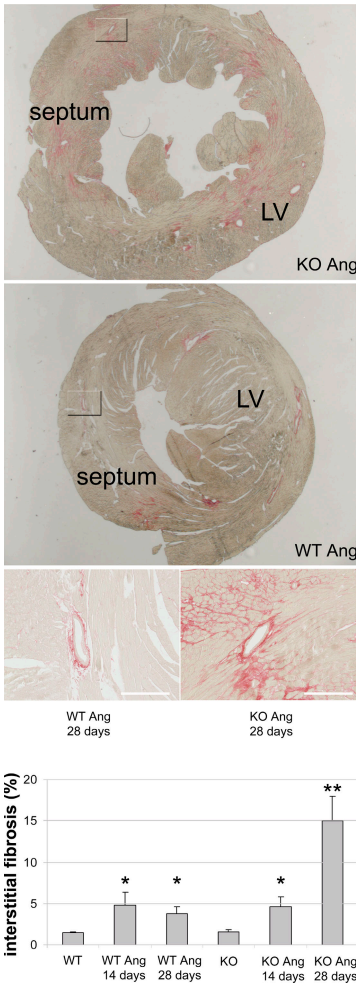

Figure 3. After 4 wk of AngII treatment, LIMP-2 KO mice have massive interstitial fibrosis. Sirius red staining of LVs of 4-wk AngII-treated LIMP-2 KO ($n = 4$) and WT ($n = 5$) mice shows marked interstitial fibrosis in KO mice (*, $P < 0.02$ vs. WT Ang and KO baseline). The overview shows that this fibrosis was not uniformly distributed, but patchy. After 2 wk of AngII treatment, LIMP-2 KO and WT mice have similar induction of interstitial fibrosis, suggesting that the massive fibrosis after 4 wk is secondary. Both KO and WT mice treated with AngII show a similar degree of perivascular fibrosis. Bars, 250 µm.

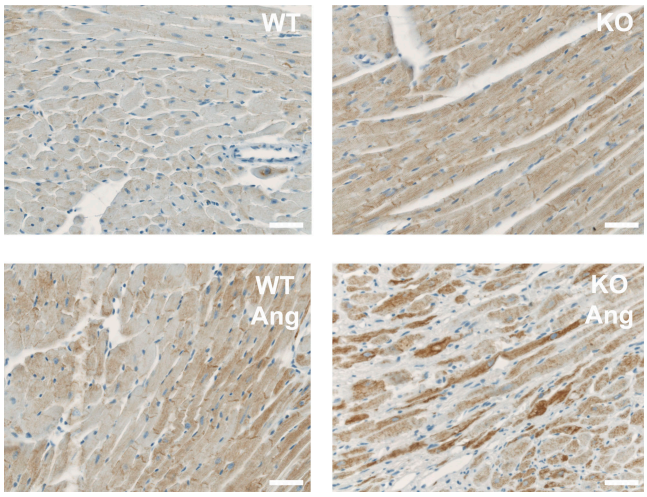

Figure 4. AngII-treated LIMP-2 KO mice have a disturbed internal architecture. Desmin-stained cardiac myocytes of AngII-treated LIMP-2 KO mice have a disturbed internal structure, as shown by the higher and more capricious desmin expression in these mice. In AngII-treated KO mice, fibrotic areas were not taken into account because here myocyte suffering is evident. Bars, 250 μm.

WTs (Fig. 2 C), reflecting the reduced size of cardiac myocytes (17). Serial echocardiography revealed that AngII induced significant cardiac dilation in AngII-treated LIMP-2 null mice already after 7 d, whereas AngII-treated WTs showed concentric LV hypertrophy without dilation (Fig. 2 D and Table S2). In addition, AngII induced loss of contractile reserve in LIMP-2 null mice as demonstrated by a reduced baseline pressure in the LV already after 2 wk of AngII treatment (Table S2) and a reduced inotropic response to dobutamine infusion after 4 wk (+dP/dt/peak systolic P 79.8/s ± 5.1 in AngII-treated KO mice vs. 100.0/s ± 4.0 in AngII-treated controls; $P < 0.005$; Fig. 2 E).

Collectively, in LIMP-2 null mice, hypertension did not induce the normal hypertrophic response but rather dilated cardiomyopathy with secondary reactive interstitial fibrosis and loss of cardiac function.

LIMP-2 expression is regulated by cardiac stress

That AngII-treated LIMP-2 null mice failed to mount a hypertrophic response, yet normally induced expression of BNP and ANF, suggested that LIMP-2 plays a crucial role in the normal response to mechanical loading. In line with this, we show that LIMP-2 expression increased significantly after cardiac myocyte stretch in vitro (Fig. 5 A). This was also seen in vivo in exercise-induced physiological hypertrophy (Fig. 5 B). LIMP-2 expression increased upon pressure loading by transverse aortic binding (Fig. 5 C). The increase in LIMP-2 occurred rapidly as LIMP-2 expression increased already after 1 h of transverse aortic binding, which shows that LIMP-2 is an early responder to cardiac loading. To assess whether LIMP-2 is also involved in the human response to cardiac pressure loading, we analyzed the expression of LIMP-2 by quantitative RT-PCR in cardiac biopsies of 20 aortic stenosis patients with overt cardiac hypertrophy and seven controls. This experiment showed a significant LIMP-2 up-regulation in the hypertrophic hearts of aortic stenosis patients as compared with controls (Fig. 5 D).

LIMP-2 is present at the cardiac ID

We next analyzed the expression pattern of LIMP-2 in pressure-overloaded murine myocardium by immunohistochemistry. The protein is expressed, as expected, in intracellular vacuole-shaped compartments of cardiac myocytes and endothelial cells, but we also found it atypically distributed on the plasma membrane of cardiac myocytes (Fig. 6 A). Immuno-electron microscopy confirmed this finding (Fig. 6 B). Strikingly, electron microscopy of AngII-treated LIMP-2 KO and control LV sections revealed abnormal morphology of the ID in LIMP-2 null mice, suggesting that LIMP-2 may be involved in normal ID biology. At cell–cell contacts, the membrane at the AngII-treated KO ID showed a significantly higher degree of convolution (Fig. 6, C and D), indicative of disturbed ID architecture (2). Because alterations in the ID have been shown to cause dilated cardiomyopathy (2, 18), we surmised that LIMP-2 may be crucial for proper functioning of the ID. Immunoprecipitation (IP) of neonatal rat cardiac myocyte protein showed that LIMP-2 physically interacts with N-cadherin, a vital constituent of adherens junctions (Fig. 7 A). We translated this finding to the human situation, as confocal microscopy of control as well as failing human myocardium confirmed the interaction between cadherin and LIMP-2 and showed that this interaction takes place at the site of the ID, where cadherin and LIMP-2 colocalize

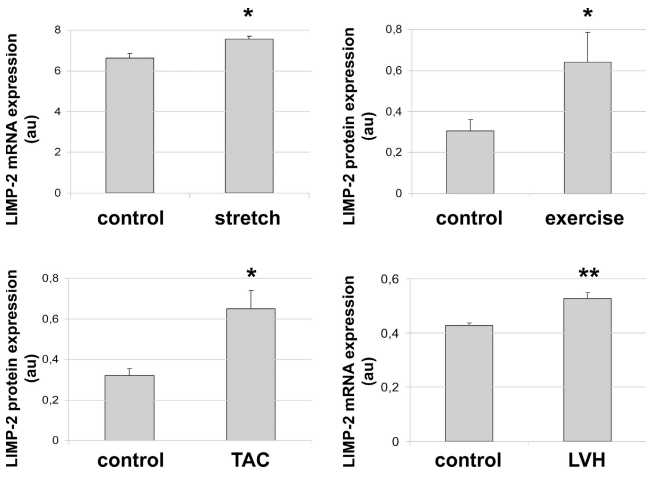

Figure 5. LIMP-2 expression is up-regulated in other forms of mechanical loading. In neonatal rat cardiac myocytes, 6 h of stretch elevated LIMP-2 mRNA expression ($n = 4$ per group) (a). LIMP-2 expression was also up-regulated in hypertrophic myocardium from rats that had undergone exercise training for 10 wk (5 d per week; $n = 6$) as compared with nonhypertrophic control rats ($n = 7$) (b). After 1 h of transverse aortic banding in mice, LIMP-2 protein is elevated (c). LIMP-2 mRNA is up-regulated in hypertrophic patients with aortic stenosis (LVH; $n = 20$) as compared with nonhypertrophic control patients ($n = 7$) (d). *, $P < 0.05$ versus control; **, $P < 0.01$ versus control; LVH; LV hypertrophy.

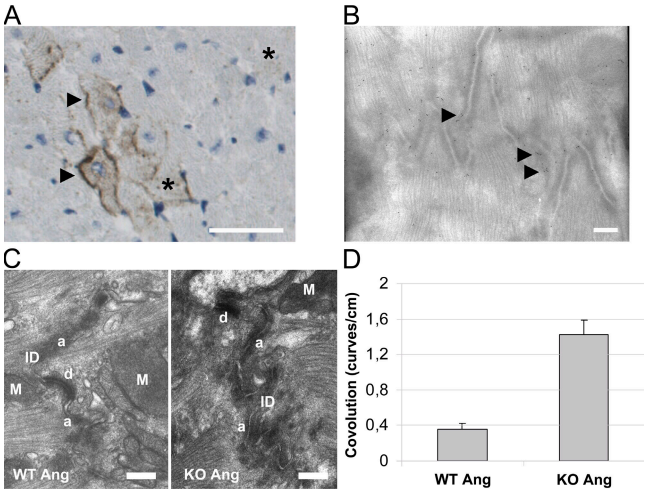

Figure 6. LIMP-2 is present at the plasma membrane of cardiac myocytes and is important for ID function. Light (A) and immunoelectron (B) microscopy on a pressure-overloaded mouse, respectively. Rat LV tissue sections show LIMP-2 staining in intracellular compartments (*) and on plasma membranes of cardiac myocytes (arrows). Bars, 250 μm (A), respectively, 1 μm (B). Electron microscopy shows normal IDs in AngII-treated WT mice, whereas in AngII-treated LIMP-2 KO mice, the IDs have a higher degree of convolution, paralleled by the dilated cardiomyopathy in these mice (C). Bars, 2 μm. Degree of convolution was quantified (blinded) by counting the number of curves per centimeter ID on electron microscopic pictures and differed significantly (*, $P < 10^{-5}$ vs. WT AngII; $n = 15$ for WT AngII and $n = 15$ for KO AngII) (D). M, mitochondrion; a, adherens junction; d, desmosome.

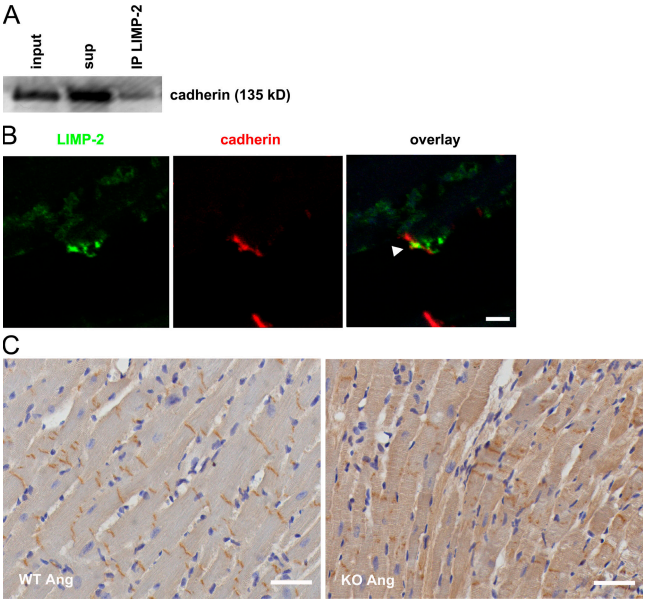

Figure 7. LIMP-2 regulates cadherin distribution. (A) LIMP-2 binds to cadherin in neonatal rat ventricular myocytes. LIMP-2 was immunoprecipitated (IP), and cadherin was immunoblotted (IB) in the total cell lysate (input), the supernatant (sup), and the precipitated protein lysate (IP). Part of the cadherin protein content of cardiac myocytes is bound by LIMP-2. (B) Representative tissue section of an HF patient was immunofluorescently stained with anti–pan-cadherin (red) and anti–LIMP-2 (green). The arrow shows colocalization of LIMP-2 and cadherin at the ID of cardiac myocytes. Bar, 50 μm. Tissue sections of AngII-treated LIMP-2 KO and WT LVs were immunostained with anti–pan-cadherin (C). In WT mice, the cadherin distribution is confined to the IDs yielding a regular appearance of cadherin, whereas in LIMP-2 KO mice, the localization of cadherin has lost the typical pattern produced by a strict location at the ID. Bars, 250 μm.

(Fig. 7 B and Fig. S2 and Videos S1 and S2, which are available at http://www.jem.org/cgi/content/full/jem.20070145/DC1). This suggested that LIMP-2 may be important for proper ID function by mediating the role of cadherin. Indeed, histochemical analysis of cadherin in the hearts of LIMP-2 null mice showed aberrant cadherin distribution (Fig. 7 C) but normal distribution in AngII-treated WTs. AngII-treated WT mice show cadherin expression at the contact sites between two longitudinal cardiac myocytes, whereas this expression is less organized and more diffuse in the cardiac myocytes of AngII-treated LIMP-2 KO mice. This disturbed localization was not seen for another member of the ID, connexin 43 (Fig. S3). These data suggest that LIMP-2 is important for the proper structural organization of the ID.

LIMP-2 regulates ID integrity

The functional integrity of the ID depends on the proper interaction between P(Ser37)-β-catenin and cadherin (19, 20). Therefore, we investigated whether the absence of LIMP-2 affected the binding of P-β-catenin to cadherin. IP of cadherin in LV lysates of LIMP-2 KO and control mice showed that the absence of LIMP-2 indeed diminished the interaction between P-β-catenin and cadherin (Fig. 8, A and D). This mechanism was independently confirmed in another model of LIMP-2 inactivation in which we introduced short-hairpin RNA (shRNA) against LIMP-2 (shLIMP-2) with a lentiviral vector to neonatal rat cardiac myocytes. After 10 d of culture, LIMP-2 protein expression was diminished by 92% in shLIMP-2–treated cardiac myocytes as compared with control-treated cardiac myocytes (Fig. 8 B). Again, there was a diminished interaction between P-β-catenin and cadherin in the absence of LIMP-2 (Fig. 8, C and D). IP was specific for cadherin (Fig. S4, available at http://www.jem.org/cgi/content/full/jem.20070145/DC1).

To further establish the role of LIMP-2 in the binding of P-β-catenin to cadherin, we asked whether overexpression of LIMP-2 would increase the levels of cadherin-bound P-β-catenin. Indeed, 513-fold overexpression of LIMP-2 in neonatal rat cardiac myocytes increased the amount of P-β-catenin bound to cadherin (Fig. 8, E and F), confirming that LIMP-2 modulates the interaction between P-β-catenin and cadherin.

DISCUSSION

We demonstrate in this study that the lysosomal protein LIMP-2 is an important and novel component of the cardiac myocyte ID, in particular adherens junctions. We show that LIMP-2 binds to N-cadherin and that LIMP-2 null mice fail to mount a hypertrophic response to pressure loading but develop dilated cardiomyopathy upon AngII-induced hypertension, which

is accompanied by disturbed localization of N-cadherin and reduced affinity of β-catenin for N-cadherin in the heart. Confirming this in vitro, we show that knockdown of LIMP-2 in cultured myocytes also disturbs interactions between N-cadherin and β-catenin, whereas LIMP-2 overexpression has the opposite effect. This suggests that LIMP-2, which was initially known as a lysosomal protein, is also an important part of the ID and is crucial for the hypertrophic response to cardiac loading.

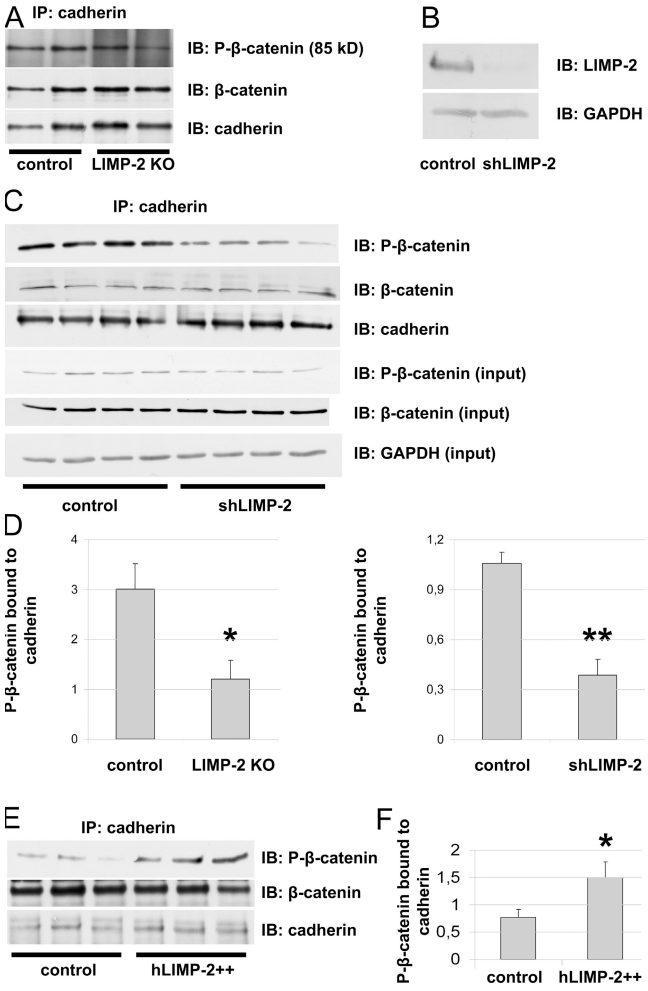

Figure 8. LIMP-2 regulates ID integrity by regulating the binding of phosphorylated β-catenin to cadherin. Immunoblot (IB) of lysates of neonatal rat cardiac myocytes that were treated either with shLIMP-2 or control shRNA (B). After 10 d of culture, cardiac myocytes show a 92% knockdown of LIMP-2 protein. Equal protein loading was confirmed by GAPDH. Representative immunoblots (IB) show diminished levels of P-β-catenin after IP with anti–pan-cadherin in LIMP-2 KO tissue lysates (A) as well as in shLIMP-2 cell lysates (C) as compared with control. P-β-catenin in total shLIMP-2 and control protein lysates was comparable (C). Quantification of immunoblots ($n = 3$ per group for control and LIMP-2 KO tissue lysates; $n = 4$ per group for control and shLIMP-2 cell lysates) is shown in D. Overexpression of LIMP-2 in neonatal rat cardiac myocytes increases levels of P-β-catenin bound to pan-cadherin (E and F). *, $P < 0.05$ versus control; **, $P < 0.001$ versus control.

LIMP-2 is a novel mediator of ID function

LIMP-2 stands out among ID proteins. Complete loss of other major constituents of the ID (cadherin, β-catenin, and plakoglobin) is lethal due to the developmental cardiac derangements (3–6), suggesting that these components of the ID are essential for normal cardiac development. In contrast, cardiac development is normal in LIMP-2 null mice, and loss of LIMP-2 only affects postnatal cardiac remodeling upon hypertension. This suggests that LIMP-2 represents a different type of ID protein, whose role is essential mainly under increased loading conditions. A protective role for LIMP-2 against excessive loading is suggested by our finding that LIMP-2 null mice developed cardiac dilation and secondary excessive fibrosis in response to pressure loading by chronic AngII infusion. This specific role for LIMP-2 is underlined by our finding that expression of LIMP-2 further rises in hypertrophied rat hearts that are on the brink of progression to HF, which suggests that LIMP-2 expression particularly increases in cardiac myocytes that are incapable of normalizing loading conditions. This is also underlined by our finding that LIMP-2 expression increases rapidly with pressure loading, and also increases with exercise-induced physiological loading. We translated these findings to the human situation, which showed that LIMP-2 is also robustly increased in patients with clinically severe pressure loading. Collectively, we suggest that LIMP-2 is a novel mediator of ID function and represents a hitherto unidentified class of mediators that are essential in the hypertrophic response to increased cardiac loading.

Mechanisms of LIMP-2–mediated response to loading

We documented ID abnormalities in pressure-loaded LIMP-2 null mice. Remodeling of the ID has been shown previously during the transition from compensated LV hypertrophy toward HF (19), whereas structural perturbations of the ID have been linked to dilated cardiomyopathy in humans, hamsters, and pigs (2, 18, 21). We show that LIMP-2 binds N-cadherin, suggesting a role for LIMP-2 via this ID constituent. Indeed, pressure-overloaded LIMP-2 KO mice show abnormal IDs on electron microscopy and their N-cadherin distribution is disturbed, suggesting a defect in the adherens junctions. The strength of adherens junctions is determined by the binding affinity between N-cadherin and β-catenin (22), which is regulated by phosphorylation of the latter (19, 20). We show in vivo as well as in vitro that loss of LIMP-2 disturbs this N-cadherin–β-catenin complex. Given the linkage of adherens junctions to myofibrils, a loss of LIMP-2 is expected to lead to a decreased force transduction efficiency across the plasma membrane (18). The importance of the level of LIMP-2 is underlined by our finding that in vitro overexpression of LIMP-2 increases the binding of N-cadherin to β-catenin. This suggests that the increased LIMP-2 expression in failure-prone hypertrophy has protective purposes and is able to improve the N-cadherin–β-catenin interaction.

We suggest that LIMP-2 is essential for the proper binding of N-cadherin to β-catenin and that this role is particularly important under loading conditions. However, the precise

way by which LIMP-2 assures the binding of N-cadherin to β-catenin remains to be elucidated. LIMP-2 contains two transmembrane domains, a cytoplasmic loop and two luminal glycosylated domains (23). It is known that lysosomal membrane proteins can shuttle between lysosomal and plasma membranes. A recent study by Knipper et al. (24) shows LIMP-2 playing a significant role in the cell surface expression of ion channels in the ear. In addition, LIMP-2 can bind to TSP1 (13) and TSP2 (not depicted). This latter is intriguing, as we have documented earlier that TSP2 is also essential for the response to cardiac pressure loading and increases in failure-prone forms of LV hypertrophy (10). This suggests that both LIMP-2 and TSP2 may be part of a complex that is needed for the cardiac myocyte to mount an adaptive response to loading.

Implications

We uncover a novel role for LIMP-2 as an important mediator of the ID when the myocardium faces increased loading conditions. Apart from this novel biological insight, our finding that expression of LIMP-2 rises in hypertrophied rat hearts that are on the brink of progression to HF makes it tempting to speculate that increased LIMP-2 expression by cardiac myocytes demonstrates their inability to normalize loading conditions. As such, increased LIMP-2 expression may signify that normalization of cardiac loading conditions by hypertrophy has failed, and that the ID is signaling to invoke a continued hypertrophic response. Because we show that LIMP-2 expression is also robustly increased in patients with clinically severe pressure loading and is located at the plasma membrane, LIMP-2 may be an attractive target for molecular imaging to identify—already in a very early stage—the myocardium that is about to succumb to the pressure.

MATERIALS AND METHODS

Ren-2 rats, microarray analysis, and immunoblotting. From 10-wk-old Ren-2 and Sprague-Dawley rats (Möllegard), a biopsy of the LV was taken as described previously (12). Rats were followed by serial echocardiography at 10, 12, 15, 16, 18, 19, and 21 wk of age and killed at 15–18 wk upon clinical signs of HF (HF-prone/ HF-prone rats) or at 21 wk when clinical signs of failure had not appeared (compensated/compensated rats). Total RNA was isolated from LV biopsies and amplified as described previously (10, 25), hybridized to Affymetrix rat RAE230 2.0 GeneChips, and analyzed with Microarray Analysis Suite software (version 5.0). 50 μg of LV protein extracts were immunoblotted with polyclonal rabbit anti–LIMP-2 (1:500; Novus Biologicals) and polyclonal rabbit anti-GAPDH (1:10,000; Abcam).

LIMP-2 KO mice. 10–12-wk-old male LIMP-2 KO and WT C57/Bl6 mice weighing 20–25 g were used. To study the blood pressure effects of AngII, arterial pressures were monitored during intravenous infusions at doses of 0.5, 1.5, 5, 15, and 50 ng per minute. To study the development of LV hypertrophy, AngII (1.5 μg/g/day; Bachem AG) was infused subcutaneously by osmotic minipump 2004 (Alzet) for 14 and 28 d. Echocardiography was performed at days 0, 7, 10, 14, and 28. At days 14 and 28, mice were hemodynamically monitored (dP/dt) using a Millar pressure sensor under basal- and dobutamin-stimulated conditions, and then LVs were removed. RNA was isolated with an RNeasy mini kit (QIAGEN), and SYBR Green quantitative RT-PCR analysis was performed on a BioRad iCycler to determine BNP, ANF, and aska expression (Table I).

LV sections were stained with Picro Sirious red and hematoxylin and eosin as described previously (26), or were immunohistochemically stained with monoclonal mouse anti–pan-cadherin (1:500; Sigma-Aldrich), monoclonal

Table I. List of primers for SYBR Green PCR and for shLIMP-2 production

Gene	Primer	Sequence
Mouse-BNP	F	5′-GTTTGGGCTGTAACGCACTGA-3′
	R	5′-GAAAGAGACCCAGGCAGAGTCA-3′
Mouse-ANF	F	5′-ATTGACAGGATTGGAGCCCAGAGT-3′
	R	5′-TGACACACCACAAGGGCTTAGGAT-3′
Mouse-aska	F	5′-TGAGACCACCTACAACAGCA-3′
	R	5′-CCAGAGCTGTGATCTCCTTC-3′
Mouse-PPIA[a]	F	5′-CAAATGCTGGACCAAACACAA-3′
	R	5′-GCCATCCAGCCATTCAGTCT-3′
Human–LIMP-2	F	5′-GTTTGGGCTGTAACGCACTGA-3′
	R	5′-GAAAGAGACCCAGGCAGAGTCA-3′
Human-GAPDH[a]	F	5′-ACCCACTCCTCCACCTTTGAC-3′
	R	5′-ACCCTGTTGCTGTAGCCAAATT-3′
Rat–LIMP-2	F	5′-TGCGTCCAAACAAGGAAGAAC-3′
	R	5′-AATCTCTTGGCCCCTCTTAAAATAA-3′
Rat–PGK-1[a]	F	5′-CGGAGACACCGCCACTTG-3′
	R	5′-AAGGCAGGAAAATACTAAACATTGC-3′
Rat–shLIMP-2[b]	Sense	5′-GGAAGAACATGAGTCATTT**GTCAAGAGA**AAATGACTCATGTTCTTCCTTTTTC-3′
	Antisense	5′-TCGAGAAAAAGGAAGAACATGAGTCATTT**TCTCTTGAC**AAATGACTCATGTTCTTCC-3′

[a]Housekeeping genes: PPIA, cyclophilin A; GAPDH, glyceraldehyde 3-phosphate dehydrogenase; PGK-1, phosphoglycerate kinase 1.
[b]Rat–shLIMP-2 oligonucleotides; hairpin structure in bold.

mouse anti–human desmin (1:50; DakoCytomation), and polyclonal rabbit anti–rat connexin 43 (Abcam). Ultrastructural analysis was performed by transmission electron microscopy as described previously (10).

LV protein extracts were immunoprecipitated with monoclonal mouse anti–pan-cadherin (1:100; Sigma-Aldrich) or IgG. IP lysates were immunoblotted with monoclonal anti–pan-cadherin (1:5,000), polyclonal anti–P-β-catenin (1:1,000; Ser33/37/Thr41; Cell Signaling Technology), and monoclonal anti–β-catenin (1:1,000; BD Transduction Laboratories).

LIMP-2 in mice with transverse aortic binding and in aortic stenosis. 12-wk-old C57/Bl6 mice were subjected to transverse aortic binding or sham surgery for 1 h or 1 d. 50 μg of LV protein extracts were immunoblotted with LIMP-2 and GAPDH antibodies as described above.

RNA was isolated from transmural biopsies obtained from 20 aortic stenosis patients and seven nonhypertrophic control patients as described previously (25), and SYBR Green quantitative PCR analysis was performed to determine LIMP-2 expression (Table I).

Double immunofluorescent stainings with rabbit anti–LIMP-2 (1:250; Cy2) and mouse anti–pan-cadherin (1:500; Cy3) were performed on sections of a human control and a patient that died of overt HF, as defined by an ejection fraction of <35%. Nuclear counterparts were stained with Topro-3 (Invitrogen). Sections were imaged with a laser scanning confocal system (Leica), digitized at a final magnification of 126, and analyzed with Leica confocal software. The ethics committees of the Academic Hospital Maastricht and of University Hospital Leuven approved the study, and all patients gave informed consent.

Cell culture and lentiviral vectors. A rat LIMP-2 shRNA-expressing lentiviral vector was generated by annealing complementary shLIMP-2 oligonucleotides (Table I) and ligating them into HpaI- and XhoI-digested pLL3.7 puro vector DNA (modified from a donation by L. van Parijs, Massachusetts Institute of Technology, Cambridge, MA). Lentiviral production was performed by cotransfection of 3 μg shLIMP-2/pLL3.7 puro or empty pLL3.7puro and packaging vectors into 293FT cells by Lipofectamine 2000 (Invitrogen), and virus-containing supernatant was harvested after 48 h.

A human LIMP-2 full-length cDNA-expressing lentiviral vector was generated by cloning the human LIMP-2 cDNA into XbaI- and EcoRI-digested pCDH1-MCS1-EF1-Puro Vector (System Biosciences). Lentiviral production was performed by cotransfection of 3 μg hLIMP-2/pCDH1-MCS1-EF1-puro or empty pCDH1-MCS1-EF1-puro and packaging vectors into 293FT cells by Lipofectamine 2000 (Invitrogen), and virus-containing supernatant was harvested after 48 h.

Rat ventricular cardiac myocytes (RCMs) were isolated by enzymatic disassociation of 1- to 2-d-old neonatal rats as described previously (27). For lentiviral infection and subsequent IP or RNA isolation, 5×10^5 RCMs per well were plated on gelatinized six-well plates and cultured overnight in DMEM/M199 (4:1) media supplemented with 10% horse serum, 5% newborn calf serum, glucose, gentamycin, and AraC. The next day, RCMs were placed on low serum media and infected with shLIMP-2/pLL3.7, hLIMP-2/pCDH, or empty lentivirus, facilitated by polybrene (Sigma-Aldrich). After puromycin selection (3 μg/ml), infection efficiencies were above 80%. After 10 d of culture, cellular protein was isolated for IP with anti–LIMP-2 (1:100), monoclonal mouse anti–pan-cadherin (Sigma-Aldrich; 1:100), or IgG. IP lysates were immunoblotted as described above.

For stretch experiments, RCMs were cultured on a collagen type I–coated silastic membrane (Specialty Manufacturing, Inc.) and subjected to static, equibiaxial stretch during 6 h. RNA was isolated with an RNeasy mini kit (QIAGEN) for LIMP-2 SYBR Green quantitative RT-PCR (Table I).

All study protocols involving animal experiments were approved by the Animal Care and Use Committee of the Universiteit Maastricht and were performed according to the official rules formulated in the Dutch law on care and use of experimental animals, highly similar to those of the National Institutes of Health.

Statistical analyses. Data are presented as average ± SEM. The data for each study group were compared using the Mann-Whitney or Student's *t* test where appropriate. $P < 0.05$ was considered to be statistically significant.

Online supplemental material. In Table S1, a list is presented of genes differentially expressed in failure-prone as compared with compensated Ren-2 rats. The differential expression of these genes precedes the development of HF in Ren-2 rats because it is derived from cardiac biopsies taken at 10 wk of age, when all rats still have compensatory hypertrophy. In Table S2, elaborate echocardiographic data are presented of LIMP-2 WT and KO mice at baseline and after 14 and 28 d of AngII treatment. Fig. S1 shows cardiac sections stained for desmin after AngII treatment in LIMP-2 WT and KO mice. This figure shows additional examples besides the example that was given in Fig. 4. Fig. S2 presents immunofluorescent stainings of human failing and control hearts with anti–pan-cadherin (red) and anti–LIMP-2 (green). This figure shows additional photographs to Fig. 7. Fig. S3 shows normal expression of connexin 43 at the ID of AngII-treated LIMP-2 KO and WT mice. In Fig. S4, we show that IP in Fig. 8 is specific for cadherin. Videos S1 and S2 present an interactive three-dimensional reconstruction of LIMP-2 bound to and colocalized with cadherin in the human heart. The supplemental material is available at http://www.jem.org/cgi/conent/full/jem.20070145/DC1.

We are grateful to Dr. Jacq Cleutjens and Dr. Leon de Windt for support regarding the histological analyses, to Hans Duimel for his expertise in electron microscopy, and to Melissa Swinnen, Agnieszka Strzelecka, and Davy van Houten for surgical assistance. We thank Dr. Matthijs Blankesteijn for kindly providing us with β-catenin antibodies.

This study was supported by a VIDI grant (016.036.346) from the Netherlands Organisation for Scientific Research (NWO) to Y.M. Pinto, by Netherlands Heart Foundation grant 2003T302, and by the Deutsche Forschungsgemeinschaft SA683/5-1 to P. Saftig. Y.M. Pinto is an established investigator of the Netherlands Heart Foundation.

The authors have no conflicting financial interests.

Submitted: 17 January 2007
Accepted: 16 April 2007

REFERENCES

1. Opie, L.H. 2006. Controversies in cardiology. *Lancet*. 367:13–14.
2. Perriard, J.C., A. Hirschy, and E. Ehler. 2003. Dilated cardiomyopathy: a disease of the intercalated disc? *Trends Cardiovasc. Med*. 13:30–38.
3. Radice, G.L., H. Rayburn, H. Matsunami, K.A. Knudsen, M. Takeichi, and R.O. Hynes. 1997. Developmental defects in mouse embryos lacking N-cadherin. *Dev. Biol*. 181:64–78.
4. Ruiz, P., V. Brinkmann, B. Ledermann, M. Behrend, C. Grund, C. Thalhammer, F. Vogel, C. Birchmeier, U. Gunthert, W.W. Franke, and W. Birchmeier. 1996. Targeted mutation of plakoglobin in mice reveals essential functions of desmosomes in the embryonic heart. *J. Cell Biol*. 135:215–225.
5. Haegel, H., L. Larue, M. Ohsugi, L. Fedorov, K. Herrenknecht, and R. Kemler. 1995. Lack of beta-catenin affects mouse development at gastrulation. *Development*. 121:3529–3537.
6. Isac, C.M., P. Ruiz, B. Pfitzmaier, H. Haase, W. Birchmeier, and I. Morano. 1999. Plakoglobin is essential for myocardial compliance but dispensable for myofibril insertion into adherens junctions. *J. Cell. Biochem*. 72:8–15.
7. Franz, W.M., O.J. Muller, and H.A. Katus. 2001. Cardiomyopathies: from genetics to the prospect of treatment. *Lancet*. 358:1627–1637.
8. Norgett, E.E., S.J. Hatsell, L. Carvajal-Huerta, J.C. Cabezas, J. Common, P.E. Purkis, N. Whittock, I.M. Leigh, H.P. Stevens, and D.P. Kelsell. 2000. Recessive mutation in desmoplakin disrupts desmoplakin-intermediate filament interactions and causes dilated cardiomyopathy, woolly hair and keratoderma. *Hum. Mol. Genet*. 9:2761–2766.
9. van Tintelen, J.P., M.M. Entius, Z.A. Bhuiyan, R. Jongbloed, A.C. Wiesfeld, A.A. Wilde, J. van der Smagt, L.G. Boven, M.M. Mannens, I.M. van Langen, et al. 2006. Plakophilin-2 mutations are the major

determinant of familial arrhythmogenic right ventricular dysplasia/cardiomyopathy. *Circulation*. 113:1650–1658.
10. Schroen, B., S. Heymans, U. Sharma, W.M. Blankesteijn, S. Pokharel, J.P. Cleutjens, J.G. Porter, C.T. Evelo, R. Duisters, R.E. van Leeuwen, et al. 2004. Thrombospondin-2 is essential for myocardial matrix integrity: increased expression identifies failure-prone cardiac hypertrophy. *Circ. Res*. 95:515–522.
11. Sharma, U.C., S. Pokharel, T.J. van Brakel, J.H. van Berlo, J.P. Cleutjens, B. Schroen, S. Andre, H.J. Crijns, H.J. Gabius, J. Maessen, and Y.M. Pinto. 2004. Galectin-3 marks activated macrophages in failure-prone hypertrophied hearts and contributes to cardiac dysfunction. *Circulation*. 110:3121–3128.
12. van Haaften, R.I., B. Schroen, B.J. Janssen, A. van Erk, J.J. Debets, H.J. Smeets, J.F. Smits, A. van den Wijngaard, Y.M. Pinto, and C.T. Evelo. 2006. Biologically relevant effects of mRNA amplification on gene expression profiles. *BMC Bioinformatics*. 7:200.
13. Crombie, R., and R. Silverstein. 1998. Lysosomal integral membrane protein II binds thrombospondin-1. Structure-function homology with the cell adhesion molecule CD36 defines a conserved recognition motif. *J. Biol. Chem*. 273:4855–4863.
14. Eskelinen, E.L., Y. Tanaka, and P. Saftig. 2003. At the acidic edge: emerging functions for lysosomal membrane proteins. *Trends Cell Biol*. 13:137–145.
15. Nishino, I., J. Fu, K. Tanji, T. Yamada, S. Shimojo, T. Koori, M. Mora, J.E. Riggs, S.J. Oh, Y. Koga, et al. 2000. Primary LAMP-2 deficiency causes X-linked vacuolar cardiomyopathy and myopathy (Danon disease). *Nature*. 406:906–910.
16. Stypmann, J., K. Glaser, W. Roth, D.J. Tobin, I. Petermann, R. Matthias, G. Monnig, W. Haverkamp, G. Breithardt, W. Schmahl, et al. 2002. Dilated cardiomyopathy in mice deficient for the lysosomal cysteine peptidase cathepsin L. *Proc. Natl. Acad. Sci. USA*. 99:6234–6239.
17. Stilli, D., L. Bocchi, R. Berni, M. Zaniboni, F. Cacciani, C. Chaponnier, E. Musso, G. Gabbiani, and S. Clement. 2006. Correlation of alpha-skeletal actin expression, ventricular fibrosis and heart function with the degree of pressure overload cardiac hypertrophy in rats. *Exp. Physiol*. 91:571–580.
18. Ferreira-Cornwell, M.C., Y. Luo, N. Narula, J.M. Lenox, M. Lieberman, and G.L. Radice. 2002. Remodeling the intercalated disc leads to cardiomyopathy in mice misexpressing cadherins in the heart. *J. Cell Sci*. 115:1623–1634.
19. Wang, X., and A.M. Gerdes. 1999. Chronic pressure overload cardiac hypertrophy and failure in guinea pigs: III. Intercalated disc remodeling. *J. Mol. Cell. Cardiol*. 31:333–343.
20. Tsybouleva, N., L. Zhang, S. Chen, R. Patel, S. Lutucuta, S. Nemoto, G. DeFreitas, M. Entman, B.A. Carabello, R. Roberts, and A.J. Marian. 2004. Aldosterone, through novel signaling proteins, is a fundamental molecular bridge between the genetic defect and the cardiac phenotype of hypertrophic cardiomyopathy. *Circulation*. 109:1284–1291.
21. Fujio, Y., F. Yamada-Honda, N. Sato, H. Funai, A. Wada, N. Awata, and N. Shibata. 1995. Disruption of cell-cell adhesion in an inbred strain of hereditary cardiomyopathic hamster (Biol. 14.6). *Cardiovasc. Res*. 30:899–904.
22. Gumbiner, B.M. 2000. Regulation of cadherin adhesive activity. *J. Cell Biol*. 148:399–404.
23. Gamp, A.C., Y. Tanaka, R. Lullmann-Rauch, D. Wittke, R. D'Hooge, P.P. De Deyn, T. Moser, H. Maier, D. Hartmann, K. Reiss, et al. 2003. LIMP-2/LGP85 deficiency causes ureteric pelvic junction obstruction, deafness and peripheral neuropathy in mice. *Hum. Mol. Genet*. 12:631–646.
24. Knipper, M., C. Claussen, L. Ruttiger, U. Zimmermann, R. Lullmann-Rauch, E.L. Eskelinen, J. Schroder, M. Schwake, and P. Saftig. 2006. Deafness in LIMP2-deficient mice due to early loss of the potassium channel KCNQ1/KCNE1 in marginal cells of the stria vascularis. *J. Physiol*. 576:73–86.
25. Heymans, S., B. Schroen, P. Vermeersch, H. Milting, F. Gao, A. Kassner, H. Gillijns, P. Herijgers, W. Flameng, P. Carmeliet, et al. 2005. Increased cardiac expression of tissue inhibitor of metalloproteinase-1 and tissue inhibitor of metalloproteinase-2 is related to cardiac fibrosis and dysfunction in the chronic pressure-overloaded human heart. *Circulation*. 112:1136–1144.
26. Junqueira, L.C., G. Bignolas, and R.R. Brentani. 1979. Picrosirius staining plus polarization microscopy, a specific method for collagen detection in tissue sections. *Histochem. J*. 11:447–455.
27. De Windt, L.J., P.H. Willemsen, S. Popping, G.J. Van der Vusse, R.S. Reneman, and M. Van Bilsen. 1997. Cloning and cellular distribution of a group II phospholipase A2 expressed in the heart. *J. Mol. Cell. Cardiol*. 29:2095–2106.